

Multifractality in complex networks

Dan-Ling Wang¹, Zu-Guo Yu^{1,2*} and Vo Anh¹

¹Discipline of Mathematical Sciences, Faculty of Science and Technology,
Queensland University of Technology, Brisbane, Q4001, Australia.

²School of Mathematics and Computational Science, Xiangtan University, Hunan 411105, China.

Abstract

Complex networks have recently attracted much attention in diverse areas of science and technology. Many networks such as the WWW and biological networks are known to display spatial heterogeneity which can be characterized by their fractal dimensions. Multifractal analysis is a useful way to systematically describe the spatial heterogeneity of both theoretical and experimental fractal patterns. In this paper, we propose a new box covering algorithm for multifractal analysis of complex networks. This algorithm is used to calculate the generalized fractal dimensions D_q of some theoretical networks, namely scale-free networks, small world networks and random networks, and one kind of real networks, namely protein-protein interaction (PPI) networks of different species. Our numerical results indicate the existence of multifractality in scale-free networks and PPI networks, while the multifractal behavior is not clear-cut for small world networks and random networks. The possible variation of D_q due to changes in the parameters of the theoretical network models is also discussed.

Key words: Complex networks; multifractality; box covering algorithm.

PACS numbers: 05.45.Df, 47.53.+n, 89.75.Hc

1 Introduction

Complex networks have been studied extensively due to their relevance to many real-world systems such as the world-wide web, the internet, energy landscapes, and biological and social systems [1].

It has been shown that many real complex networks share distinct characteristics that differ in many ways from random and regular networks [2, 3]. Three fundamental properties of real complex networks have attracted much attention recently: the small-world property [4, 5], the scale-free property [6-8], and the self-similarity [1]. The small-world property means that the

*Corresponding author, e-mail: yuzg@hotmail.com

average shortest path length between vertices in the network is short, usually scaling logarithmically with the size N of the network [3]. A famous example is the so-called *six degrees of separation* in social networks [5]. A large number of real networks are referred to as *scale-free* because the probability distribution $P(k)$ of the number of links per node (also known as the degree distribution) satisfies a power law $P(k) \sim k^{-\gamma}$ with the degree exponent γ varying in the range $2 < \gamma < 3$ [6]. In view of their small-world property, it was believed that complex networks are not self-similar under a length-scale transformation. After analyzing a variety of real complex networks, Song *et al.* [1] found that they consist of self-repeating patterns on all length scales, i.e., they have *self-similar structures*. In order to unfold the self-similar property of complex networks, Song *et al.* [1] calculated their fractal dimension, a known useful characteristic of complex fractal sets [9-11], and found that the box-counting method is a proper tool for further investigations of network properties. Because a concept of metric on graphs is not as straightforward as the Euclidean metric on Euclidean spaces, the computation of the fractal dimension of networks via a box-counting approach is much more complicated than the traditional box-counting algorithm for fractal sets in Euclidean spaces. Song *et al.* [12] developed a more involved algorithm to calculate the fractal dimension of complex networks. Then Kim *et al.* [13] proposed an improved algorithm by considering the skeleton of networks. Zhou *et al.* [14] proposed an alternative algorithm, based on the edge-covering box counting, to explore the self-similarity of complex cellular networks. Later on, a ball-covering approach [15] and an approach defined by the scaling property of the volume [3, 16] were proposed for calculating the fractal dimension of complex networks.

The tools of fractal analysis provide a global description of the heterogeneity of an object, such as its fractal dimension. This approach is not adequate when the object may exhibit a multifractal behavior. Multifractal analysis is a useful way to systematically characterize the spatial heterogeneity of both theoretical and experimental fractal patterns [17, 18]. It was initially proposed to treat turbulence data, and has recently been applied successfully in many different fields including time series analysis [19], financial modelling [20], biological systems [21-28] and geophysical systems [29-34]. For complex networks, Lee and Jung [2] found that their behaviour is best described by a multifractal approach. As mentioned above, through the recent works by Song *et al.* [1], Guo and Cai [3], Kim *et al.* [13], Zhou *et al.* [14], Gao *et al.* [15], it was already a big step to go from the computation of the fractal dimension of a geometrical object to that of a network via the box-counting approach of fractal analysis. In this paper, we propose a new box-covering algorithm to compute the generalised fractal dimensions of a network. This is the next step to move from fractal analysis to multifractal analysis of complex networks.

We first adapt the random sequential box covering algorithm [13] to calculate the fractal dimension of the human protein-protein interaction network as well as that of its skeleton.

We next propose a box covering algorithm for multifractal analysis of networks in Section 2. This algorithm is then used to calculate in Section 3 the generalized fractal dimensions D_q of generated examples of three classes of theoretical networks, namely scale-free networks, small-world networks and random networks, and one kind of real networks, namely protein-protein interaction networks of different species. The methods to generate the theoretical networks are described. The multifractal behaviour of these networks based on the computed generalised fractal dimensions D_q is then discussed. The possible variation of D_q due to changes in the parameters of the theoretical network models is also investigated. Some conclusions are then drawn in Section 4.

2 Methods

In this section, we first introduce the box covering methods for calculating the fractal dimension of complex networks and the traditional fixed-size box counting algorithms used for multifractal analysis. We then present our new approach for multifractal analysis of complex networks in detail.

2.1 The box covering methods for calculation of fractal dimension

Box covering is a basic tool to estimate the fractal dimension of conventional fractal objects embedded in the Euclidean space. The Euclidean metric is not relevant for complex networks. A more natural metric is the shortest path length between two nodes, which is defined as the number of edges in a shortest path connecting them. Shortest paths play an important role in the transport and communication within a network. It is useful to represent all the shortest path lengths of a network as a matrix D in which the entry d_{ij} is the length of the shortest path from node i to node j . The maximum value in the matrix D is called the network diameter, which is the longest path between any two nodes in the network. Song *et al.* [1] studied the fractality and self-similarity of complex networks by using box covering techniques. They proposed several possible box covering algorithms [1] and applied them to a number of models and real-world networks. Kim *et al.* [13] introduced another method called the random sequential box covering method, which can be described as follows:

For a given network, let N_B be the number of boxes of radius r_B which are needed to cover the entire network. The fractal dimension d_B is then given by

$$N_B \sim r_B^{-d_B}.$$

By measuring the distribution of N_B for different box sizes, the fractal dimension d_B can be obtained by power law fitting of the distribution. This algorithm has the following steps [13]:

- (i) Select a node randomly at each step; this node serves as a seed which will be the center of a box.
- (ii) Search the network by distance r_B from the seed and cover all nodes which are found but have not been covered yet. Assign the newly covered nodes to the new box. If no newly covered nodes have been found, then this box is discarded.
- (iii) Repeat (i) and (ii) until all nodes in the network have been assigned to their respective boxes.

To obtain the *skeleton* of a complex network, we firstly need to calculate the edge betweenness of all the edges in this network. The betweenness b_i , also referred to as load [13], is defined as

$$b_i = \sum_{j,k \in N, j \neq k} \frac{n_{jk}(i)}{n_{jk}},$$

where N is the number of nodes, n_{jk} is the number of shortest paths connecting nodes j and k , while $n_{jk}(i)$ is the number of shortest paths connecting nodes j and k and passing through edge i . Similar to a minimum spanning tree, a skeleton is constructed so that edges which have the highest betweenness and do not form loops are selected [13]. The remaining edges in the original network are referred to as shortcuts that contribute to loop formation. In other words, the distance between any two nodes in the original network may increase in the skeleton. For example, in the human protein-protein interaction network, the largest distance between any two nodes in the original network is 21 while the largest distance between any two nodes in its skeleton is 27.

As an example, we used the above algorithm to estimate the fractal dimension of the human protein-protein interaction network as well as that of its skeleton. The result is shown in Fig. 1. When we applied the box covering algorithm on the skeleton, more boxes were needed for each fixed box radius r_B . The increasing rate of the number N_B of boxes varies when the size r_B of the box increases. More specifically, when r_B is smaller, the number of boxes needed is not much different for both the original network and its skeleton; but when r_B is larger, many more boxes are needed to cover the skeleton than the original network.

2.2 Algorithms for multifractal analysis of networks

Most well-known fractals such as the Cantor set, the Koch curve and the Sierpinski triangle are homogeneous since they consist of a geometrical figure repeated on an ever-reduced scale. For these objects, the fractal dimension is the same on all scales. However, real-world fractals may not be homogeneous; there is rarely an identical motif repeated on all scales. Two objects might have the same fractal dimension and yet look completely different. Real-world fractals possess rich scaling and self-similarity properties that can change from point to point, thus can

have different dimensions at different scales. The present paper investigates these properties on complex networks. Especially we develop tools to determine whether they are simple fractals or multifractals, and how different two networks could be even though they have the same fractal dimension. In other words, we aim to develop an approach for multifractal analysis of complex networks.

The most common algorithm of multifractal analysis is the fixed-size box-counting algorithm [18, 22, 25]. For a given probability measure $0 \leq \mu \leq 1$ with support set E in a metric space, we consider the partition sum

$$Z_\epsilon(q) = \sum_{\mu(B) \neq 0} [\mu(B)]^q, \quad (1)$$

where q is a real number and the sum runs over all different non-overlapping boxes B of a given size ϵ in a covering of the support E . It follows that $Z_\epsilon(q) \geq 0$ and $Z_\epsilon(0) = 1$. The mass exponent function $\tau(q)$ of the measure μ is defined by

$$\tau(q) = \lim_{\epsilon \rightarrow 0} \frac{\ln Z_\epsilon(q)}{\ln \epsilon}. \quad (2)$$

Proposition 1 *The mass exponent $\tau(q)$ is an increasing function of q .*

Proof. For $q_1 < q_2$, it follows from μ being a probability measure that $\mu(B_i)^{q_1} > \mu(B_i)^{q_2}$; thus $Z_\epsilon(q_1) > Z_\epsilon(q_2)$. Since $\ln \epsilon < 0$ when $\epsilon \rightarrow 0$, the increasing property of $\tau(q)$ follows. \square

The generalized fractal dimensions of the measure μ are defined as

$$D_q = \frac{\tau(q)}{q-1}, \quad q \neq 1, \quad (3)$$

and

$$D_q = \lim_{\epsilon \rightarrow 0} \frac{Z_{1,\epsilon}}{\ln \epsilon}, \quad (4)$$

for $q = 1$, where $Z_{(1,\epsilon)} = \sum_{\mu(B) \neq 0} \mu(B) \ln \mu(B)$.

Proposition 2 *D_q is a decreasing function of q for $q \neq 1$.*

Proof. Combining Eqs. (2) and (3) yields, for $q \neq 1$,

$$D_q = \lim_{\epsilon \rightarrow 0} \frac{\frac{1}{q-1} \ln Z_\epsilon(q)}{\ln \epsilon}. \quad (5)$$

We need to consider 3 cases:

(i) For $1 < q_1 \leq q_2 < \infty$, we have

$$0 < \frac{1}{q_2-1} \leq \frac{1}{q_1-1} < \infty \quad (6)$$

and

$$0 < Z_\epsilon(q_2) \leq Z_\epsilon(q_1) \leq 1,$$

that is,

$$\ln Z_\epsilon(q_2) \leq \ln Z_\epsilon(q_1) < 0. \quad (7)$$

From Eqs. (5) - (7), it is seen that $\frac{1}{q-1} \ln Z_\epsilon(q)$ increases as a function of q . Thus D_q decreases as a function of q since $\ln \epsilon < 0$ as $\epsilon \rightarrow 0$.

(ii) For $0 < q_1 \leq q_2 < 1$, we have

$$-\infty < \frac{1}{q_2 - 1} \leq \frac{1}{q_1 - 1} < -1$$

and

$$\frac{1}{q_2 - 1} \ln Z_\epsilon(q_2) \geq \frac{1}{q_1 - 1} \ln Z_\epsilon(q_1).$$

Thus D_q decreases as a function of q in this case.

(iii) For $-\infty < q_1 \leq q_2 < 0$, we have

$$-1 < \frac{1}{q_2 - 1} \leq \frac{1}{q_1 - 1} < 0$$

and also

$$\frac{1}{q_2 - 1} \ln Z_\epsilon(q_2) \geq \frac{1}{q_1 - 1} \ln Z_\epsilon(q_1).$$

Thus D_q also decreases as a function of q in this case. \square

For every box size ϵ , the number $\alpha = \frac{\log \mu(\epsilon)}{\log \epsilon}$, also referred to as the Hölder exponent, is the singularity strength of the box. This exponent may be interpreted as a crowding index of a measure of concentration: the greater α is, the smaller is the concentration of the measure, and vice versa. For every box size ϵ , the numbers of cells $N_\alpha(\epsilon)$ in which the Hölder exponent α has a value within the range $[\alpha, \alpha + d\alpha]$ behave like

$$N_\alpha(\epsilon) \sim \epsilon^{-f(\alpha)}.$$

The function $f(\alpha)$ signifies the Hausdorff dimension of the subset which has singularity α ; that is, $f(\alpha)$ characterizes the abundance of cells with Hölder exponent α and is called the *singularity spectrum* of the measure. The measure μ is said to be a *multifractal measure* if its singularity spectrum $f(\alpha) \neq 0$ for a range of values of α . The singularity spectrum $f(\alpha)$ and the mass exponent function $\tau(q)$ are connected via the Legendre transform: ([9])

$$\alpha(q) = \frac{d\tau(q)}{dq} \quad (8)$$

and

$$f(\alpha(q)) = q\alpha(q) - \tau(q), \quad q \in \mathbb{R}.$$

Considering the relationship between the mass exponent function $\tau(q)$ and the generalized dimension function D_q , the singularity spectrum $f(\alpha)$ contains exactly the same information as $\tau(q)$ and D_q .

Lau and Ngai [35] showed in their Proposition 3.4 (page 57) that

- (i) $\lim_{q \rightarrow \infty} D_q = \alpha_{\min}$;
- (ii) $\lim_{q \rightarrow -\infty} D_q = \alpha_{\max}$.

This result together with Proposition 2 and the definition of a multifractal measure given above lead to a method to determine the multifractality of a probability measure μ :

When $\alpha_{\min} = \alpha_{\max}$, the function D_q is constant for $q \neq 1$ and the measure μ is monofractal.

When $\alpha_{\min} \neq \alpha_{\max}$, D_q is a decreasing function of $q \neq 1$ and the measure μ is multifractal.

This method is the key element in the next section when we investigate the multifractality of a variety of networks.

The generalized fractal dimensions are estimated through a linear regression of $[\ln Z_\epsilon(q)]/(q-1)$ against $\ln \epsilon$ for $q \neq 1$, and similarly through a linear regression of $Z_{1,\epsilon}$ against $\ln \epsilon$ for $q = 1$. The value D_1 is called the information dimension and D_2 the correlation dimension, while D_0 is equal to the Hausdorff dimension.

For a network, the measure μ of each box is defined as the ratio of the number of nodes covered by the box and the total number of nodes in the network. The fixed-size box-counting algorithm of Kim et al. [13] described above could not be used to analyze the multifractal behavior of networks directly. Because the method contains a random process of selecting the position of the center of each box, this will affect the number of boxes with a fixed size. Especially, if a node with large degree (a hub) is randomly chosen, a lot more nodes could be covered, and it is an efficient way when we produce box covering. However, if a node with small degree is randomly chosen first, few nodes could be covered. As a result, the partition sum defined by Eq. (1) will change each time we proceed with box counting. We illustrate this situation in Fig. 2: We consider a network of eight nodes. In Fig. 2A, for a fixed box size $r_B = 1$, firstly node a is chosen as the center of a box and both nodes a and b are covered in the same box colored in black. Next, node f is chosen as a center of a box, and nodes b, c, d, e, g are all within a distance $r_B = 1$. Since node b has already been covered in the previous step, so nodes c, d, e, g, f are covered in the same box colored in blue. In the last step, node g is chosen as the center of a box and its neighboring node h is the only one found within a distance $r_B = 1$ not covered yet, so h is the only one covered in a box colored in red. In summary, three boxes are needed to cover the entire network. In Fig 2B, for the same fixed box size $r_B = 1$, firstly node h is chosen as the center of a box and both nodes h and g are covered in the same box colored in red. Next, node f is chosen as a center of a box, and nodes e, g are all within a distance $r_B = 1$. Since node g has already been covered in the previous step, so nodes e, f are covered in the same box colored in blue. Next, node d is then chosen as the center of a box and since its two neighbors f, g have already been covered, so d is the only one covered in a box colored in brown; likewise, node c is chosen and covered alone in the box colored in green. In the last step, node a is chosen as a center and both nodes a and b are covered within one box colored

in black. In summary, five boxes are needed to cover the entire network. In these two cases of Figs. 2A and 2B, the partition sums are different. *To avoid this effect, we propose to take the average of the partition sums over a large number of times and accordingly modify the original fixed-size box-counting algorithm into a new method. To our knowledge, this improvement is the first introduced in this approach to analyze the multifractal behavior of complex networks.*

We need to calculate the shortest-path distance matrix for each network and these matrices are the input data for fractal and multifractal analyses. We describe the procedure as follows:

- (i) Transform the pairs of edges and nodes in a network into a matrix $A_{N \times N}$, where N is the number of nodes of the network. The matrix $A_{N \times N}$ is a symmetric matrix where the elements $a_{ij} = 0$ or 1 with $a_{ij} = 1$ when there is an edge between node i and node j , while $a_{ij} = 0$ when there is no edge between them. We define that each node has no edge with itself and accordingly $a_{ii} = 0$.

Remark: $A_{N \times N}$ could be the input data for calculating the degree distribution and characteristic path length to determine whether the network possesses the properties of scale-free degree distribution and small-world effect.

- (ii) Compute the shortest path length among all the linked pairs and save these pairs into another matrix $B_{N \times N}$.

Remark: In graph theory, calculation of the shortest path is a significant problem and there are many algorithms for solving this problem. Here, in our approach, we use Dijkstra's algorithm [36] of the Matlab toolbox.

After the above steps we could use the matrix $B_{N \times N}$ as input data for multifractal analysis based on our *modified fixed-size box counting algorithm* as follows:

- (i) Initially, all the nodes in the network are marked as uncovered and no node has been chosen as a seed or center of a box.
- (ii) According to the number of nodes in the network, set $t = 1, 2, \dots, T$ appropriately. Group the nodes into T different ordered random sequences. More specifically, in each sequence, nodes which will be chosen as seed or center of a box are randomly arrayed.

Remark: T is the number of random sequences and is also the value over which we take the average of the partition sum $\overline{Z_r(q)}$. Here in our study, we set $T = 200$ for all the networks in order to compare.

- (iii) Set the size of the box in the range $r \in [1, d]$, where d is the diameter of the network.

Remark: When $r = 1$, the nodes covered within the same box must be connected to each other directly. When $r = d$, the entire network could be covered in only one box no matter which node was chosen as the center of the box.

- (iv) For each center of a box, search all the neighbors within distance r and cover all nodes which are found but have not been covered yet.
- (v) If no newly covered nodes have been found, then this box is discarded.
- (vi) For the nonempty boxes B , we define their measure as $\mu(B) = N_B/N$, where N_B is the number of nodes covered by the box B , and N is the number of nodes of the entire network.
- (vii) Repeat (iv) until all nodes are assigned to their respective boxes.
- (viii) When the process of box counting is finished, we calculate the partition sum as $Z_r(q) = \sum_{\mu(B) \neq 0} [\mu(B)]^q$ for each value of r .
- (ix) Repeat (iii) and (iv) for all the random sequences, and take the average of the partition sums $\overline{Z_r(q)} = (\sum^t Z_r(q))/T$, and then use $\overline{Z_r(q)}$ for linear regression.

Linear regression is an essential step to get the appropriate range of $r \in [r_{min}, r_{max}]$ and to get the generalized fractal dimensions D_q . In our approach, we run the linear regression of $[\ln \overline{Z_r(q)}]/(q-1)$ against $\ln(r/d)$ for $q \neq 1$, and similarly the linear regression of $\overline{Z_{1,r}}$ against $\ln(r/d)$ for $q = 1$, where $\overline{Z_{1,r}} = \sum_{\mu(B) \neq 0} \mu(B) \ln \mu(B)$ and d is the diameter of the network. An example of linear regression for the Arabidopsis thaliana PPI network is shown in Fig. 3. The numerical results show that the best fit occurs in the range $r \in (1, 9)$, hence we select this range to perform multifractal analysis and get the spectrum of generalized dimensions D_q .

After this spectrum has been obtained, we use $\Delta D(q) = \max D(q) - \lim D(q)$ to verify how D_q changes along each curve. The quantity $\Delta D(q)$ has been used in the literature to describe the density of an object. In this paper, based on our modified fixed-size box covering method, $\Delta D(q)$ can help to understand how the edge density changes in the complex network. In other words, a larger value of $\Delta D(q)$ means the edge distribution is more uneven. More specifically, for a network, edge distribution could vary from an area of hubs where edges are dense to an area where nodes are just connected with a few links.

In the following sections, we calculate the generalized fractal dimensions D_q . From the shape of D_q , we determine the multifractality of the network using the method described above. We then calculate $\Delta D(q)$ to verify how D_q changes along each curve.

3 Results and discussions

In recent years, with the development of technology, the research on networks has shifted away from the analysis of single small graphs and the properties of individual vertices or edges within such graphs to consideration of large-scale statistical properties of complex networks. Newman [37] reviewed some latest works on the structure and function of networked systems

such as the Internet, the World Wide Web, social networks and a variety of biological networks. Besides reviewing empirical studies, the author also focused on a number of statistical properties of networks including path lengths, degree distributions, clustering and resilience. In this paper, we pay attention to another aspect of networks, namely their multifractality. We aim to develop a tool based on this property to characterize and classify real-world networks.

It has been shown that many real complex networks share distinctive characteristics that differ in many ways from random and regular networks [2, 3, 37]. Fundamental properties of complex networks such small-world effect and the scale-free degree distribution have attracted much attention recently. These properties have in fact been found in many naturally occurring networks. In Subsections 3.1, 3.2 and 3.3, we generate scale-free networks using the BA model of Barabasi and Albert [38], small-world networks using the NW model of Newman and Watts [39], then random networks using the ER model of Erdős and Rényi [4] respectively. We then apply our modified fixed-size box counting algorithm to analyze the multifractal behavior of these networks.

3.1 Scale-free networks

We use the elegant and simple BA model of Barabasi and Albert [38] to generate scale-free networks. The origin of the scale-free behavior in many systems can be traced back to this BA model, which correctly predicts the emergence of scaling exponent. The BA model consists of two mechanisms : Initially, the network begins with a seed network of n nodes, where $n \geq 2$ and the degree of each node in the initial network should be at least 1, otherwise it will always remain disconnected from the rest of the network. For example, here we start with an initial network of 5 nodes. Its interaction matrix is

$$\begin{pmatrix} 0 & 1 & 0 & 0 & 1 \\ 1 & 0 & 0 & 1 & 0 \\ 0 & 0 & 0 & 1 & 0 \\ 0 & 1 & 1 & 0 & 0 \\ 1 & 0 & 0 & 0 & 0 \end{pmatrix}.$$

We then add one node to this initial network at a time. Each new node is connected to n existing nodes with a probability that is proportional to the number of links that the existing nodes already have. Formally, the probability p_i that the new node is connected to node i is

$$p_i = \frac{k_i}{\sum_j k_j}, \quad (9)$$

where k_i is the degree of node i . So hubs tend to quickly accumulate even more links, while nodes with only a few links are unlikely to be chosen as destination for a new link.

In this paper, these scale-free networks are generated based on the same seed which is the initial network of 5 nodes. For better comparison, in each step, one node will be added into the network with one link. Then we apply the modified fixed-size box counting method on them to detect their multifractal behavior.

In Fig. 4. we can see that scale-free networks are multifractal by the shape of the D_q curves. The D_q functions of these networks decrease sharply after the peak. An explanation is that, in a scale-free network, there are several nodes which are known as hubs that have a large number of edges connected to them, so the edge density around the areas near the hubs is larger than the remaining parts of the network.

We summarize the numerical results in Table 1 including the number of nodes, number of edges, diameter, power law exponent γ , maximum value of D_q , limit of D_q , and ΔD_q . From these results we could see that scale free networks with larger size (more nodes and more edges) are likely to have larger values of the maximum and limit of D_q . In other words, the function D_q increases with the size of a scale-free network. An explanation for this situation is that larger scale-free networks usually have more hubs which make the structure of the network more complex.

Scale-free networks show a power-law degree distribution of $P(k) \sim k^{-\gamma}$, where $P(k)$ is the probability of a node randomly chosen with degree k . It was shown in [6, 7] that when $\gamma < 2$, the average degree diverges; while for $\gamma > 3$, the standard deviation of the degree diverges. It has been found that the degree exponent γ usually varies in the range of $2 < \gamma < 3$ [6] for most scale-free networks. Accordingly, we computed the power-law exponent of these generated scale-free networks. The results show that there doesn't seem to be any clear relationship between power law and the maximum of D_q , limit of D_q or ΔD_q .

3.2 Small-world networks

In 1998, Watts and Strogatz [40] proposed a single-parameter small-world network model that bridges the gap between a regular network and a random graph. With the WS small-world model, one can link a regular lattice with pure random network by a semirandom network with high clustering coefficient and short average path length. Later on, Newman and Watts [39] modified the original WS model. In the NW model, instead of rewiring links between nodes, extra links called shortcuts are added between pairs of nodes chosen at random, but no links are removed from the existing network. The NW model is equivalent to the WS model for small p and sufficiently large N , but easier to proceed.

In this paper, we use the NW model as follows. Firstly, we should select three parameters: the dimension n , which is the number of nodes in a graph; the mean degree k (assumed to be an even integer), which is the number of nearest-neighbors to connect; and the probability p of adding a shortcut in a given row, where $0 \leq p \leq 1$ and $n \gg k \gg \ln(n) \gg 1$. Secondly, we follow

two steps:

- (i) Construct a regular ring lattice. For example, if the nodes are named N_0, \dots, N_{n-1} , there is an edge e_{ij} between node N_i and N_j if and only if $|i - j| \equiv K$ for $K \in [0, k/2]$;
- (ii) Add a new edge between nodes N_i and N_j with probability p .

An illustration of this generating process is given in Fig. 5. The upper left figure corresponds to the probability $p = 0$. It is a regular network containing 20 nodes and each node has two neighbors on both sides. In other words, in this regular network, each node has four edges. All the nodes and edges are shown in blue. Then we start generating small-world networks based on this regular network. The upper right figure of Fig. 5 corresponds to the probability $p = 0.1$; one edge is added into the network which is colored in black. The network then becomes a small-world network. The bottom left figure corresponds to the probability $p = 0.5$; seven black edges are added into the original regular network and it is also a small-world network. The bottom right figure corresponds to the probability $p = 1$; 10 black edges are added into the original small-world network and this time it becomes a random network.

In this paper, we firstly generated a regular network which contains 5000 nodes and 250,000 edges. Each node has 50 edges on each side. Then we apply the modified fixed-size box counting method on this regular network. The numerical results are shown in the last row of Table 2. Both the maximum value of D_q and the limit of D_q are equal to one, thus $\Delta D_q = 0$. This is because regular networks are not fractal, and they have dimension one. Secondly, for better comparison, we generated ten small-world networks based on a regular network of 5000 nodes with 5 edges on each side of a node. During the generation, when the probability p increases, more edges are added into the original regular network. Then we apply the modified fixed-size box counting method on them to detect their multifractal behavior. We summarize the numerical results in Table 2, which includes the number of nodes, number of edges, diameter, probability p (the generating parameter), maximum value of D_q and ΔD_q . These results indicate that, when p increases, more edges are added and accordingly both the maximum and limit values of D_q increase.

In Fig. 6 we can see that the D_q curve of a regular network whose probability $p = 0$ during generation is a straight line with the value of 1. The D_q curves of the other small-world networks are also approximately straight lines but with different D_q values. So these networks are not multifractal. Another interesting property is apparent when $0.03 < p < 0.2$, in which case D_q increases along with the value of p . More specifically, when p increases, more edges are added to the network, and both the maximum and limit values of D_q and limit of D_q increase. The values of ΔD_q are all within the error range, confirming that the D_q curves are straight lines.

3.3 Random networks

The Erdős-Rényi random graph model [4] is the oldest and one of the most studied techniques to generate complex networks.

We generate random networks based on the ER model [4]:

- (i) Start with N isolated nodes;
- (ii) Pick up every pair of nodes and connect them by an edge with probability p .

Usually, the results of this generation are separated subnetworks. In this work, we just consider the largest connected part as the network to work on and apply the modified fixed-size box counting method to detect their multifractal behaviors. We then summarize the numerical results in Table 3 including the number of nodes, number of edges, diameter, probability p (the generating parameter), maximum value of D_q , limit of D_q , and ΔD_q . These results indicate that there is no clear relationship between D_q and the size of the random network.

In Fig. 7, we can see that the D_q curves of random networks decrease slowly after the peak and the changes could be seen by the values of ΔD_q . This pattern occurs because, during the generating process, nodes are randomly connected with probability p , and few hubs may exist. Compared with scale-free networks, this decrease supports the claim that, in random networks, edges are distributed more symmetrically.

Remark: In the present study, we consider the generalized fractal dimensions D_q to determine whether the object is multifractal from the shape of D_q . For a monofractal system, which has the same scaling behavior at any point, D_q should be a constant independent of q , while for a multifractal, the D_q should be a non-increasing nonlinear curve as q increases. However, in our results, an anomalous behavior is observed: the D_q curves increase at the beginning when $q < 0$. This anomalous behavior has also been observed in Bos et al.[41], Smith and Lange [42], Fernández et al. [43]. Some reasons for this behavior have been suggested, including that the boxes contain few elements [43], or the small scaling regime covers less than a decade so that we cannot extrapolate the box counting results for the partition function to zero box size [41]. In encountering the anomalous spectra of D_q , we tried another method of multifractal analysis called the sand-box method, but the linear regression fittings are not satisfactory. We therefore used the modified fixed-size box counting algorithm in this research. For the purpose of detecting the multifractality of complex networks, we adopt the anomalous spectra of D_q and focus on the decreasing parts which are presented in Figs. 4 to 8.

3.4 Protein-protein interaction networks

Our fractal and multifractal analyses are based on connected networks which do not have separated parts or isolated nodes. In order to apply them to protein-protein interaction (PPI)

networks, some preparation is needed in advance. Firstly, we need to find the largest connected part of each data set. For this purpose many tools and methods could be used. In our study, we adopt the Cytoscape [44] which is an open bioinformatics software platform for visualizing molecular interaction networks and analyzing network graphs of any kind involving nodes and edges. In using Cytoscape, we could get the largest connected part of each interacting PPI data set and this connected part is the network on which fractal and multifractal analyses are performed.

The protein-protein interaction data we used here are mainly downloaded from two databases: The PPI networks of *Drosophila melanogaster* (fruit fly), *C. elegans*, *Arabidopsis thaliana* and *Schizosaccharomyces pombe* are downloaded from BioGRID [45]. The PPI networks of *S. cerevisiae* (baker's yeast), *E. coli* and *H. pylori* are download from DIP [46]. We also use the same human PPI network data as in [47].

We calculated the D_q spectra for eight PPI networks of different organisms as shown in Fig. 8. From these D_q curves, we see that all PPI networks are multifractal and there are two clear groupings of organisms based on the peak values of their D_q curves. The first group includes human, *Drosophila melanogaster*, *S. cerevisiae*, and *C. elegans*. The second group just includes two bacteria *E.coli* and *H. pylori*. We also see that the PPI networks of the eight organisms have similar shape for the D_q curves. They all increase when $q \in [0, 1]$, and reach their peak values around $q = 2$, then decrease sharply as $q > 2$ and finally reach their limit value when $q > 10$. So we can take $\lim D(q) = D(20)$ and use $\Delta D(q) = \max D(q) - \lim D(q)$ to verify how the D_q function changes along each curve. We summarize the corresponding numerical results in Table 4.

4 Conclusions

After analyzing a variety of real complex networks, Song et al. [1] found that they consist of self-repeating patterns on all length scales, i.e., complex networks have self-similar structures. They found that the box-counting method is a proper tool to unfold the self-similar properties of complex networks and to further investigate network properties.

However, describing objects by a single fractal dimension is a limitation of fractal analysis, especially when the networks exhibit a multifractal behavior. Multifractal analysis is a useful way to characterize the spatial heterogeneity of both theoretical and experimental fractal patterns. It allows the computation of a set of fractal dimensions, especially the generalized fractal dimensions D_q .

A modified algorithm for analyzing the multifractal behavior of complex networks is proposed in this paper. This algorithm is applied on generated scale-free networks, small-world networks and random networks as well as protein-protein interaction networks. The numerical results

indicate that multifractality exists in scale-free networks and PPI networks, while for small-world networks and random networks their multifractality is not clear-cut, particularly for small-world networks generated by the NW model. Furthermore, for scale-free networks, the values of D_q increase when the size of the network increases because larger scale-free networks usually have more hubs which make the structure of the network more complex. However, for random networks there is no clear relationship between D_q and the size of the network. The quantity $\Delta D(q) = \max D(q) - \lim D(q)$ has been used to investigate how D_q changes. Larger $\Delta D(q)$ means the network's edge distribution is more uneven; while smaller $\Delta D(q)$ means the network's edge distribution is more symmetrical, which is the case for random networks.

These results support that the algorithm proposed in this paper is a suitable and effective tool to perform multifractal analysis of complex networks. Especially, in conjunction with the derived quantities from D_q , the method and algorithm provide a needed tool to cluster and classify real networks such as the protein-protein interaction networks of organisms.

5 Acknowledgement

This project was supported by the Australian Research Council (Grant No. DP0559807), the Natural Science Foundation of China (Grant No. 11071282), the Chinese Program for New Century Excellent Talents in University (Grant No. NCET-08-06867), the Lotus Scholars Program of Hunan province of China, the Aid Program for Science and Technology Innovative Research Team in Higher Education Institutions of Hunan Province of China, and a China Scholarship Council–Queensland University of Technology Joint Scholarship. The authors wish to thank the Editor and the referees for their comments and suggestions to improve the paper.

References

- [1] C. Song, S. Havlin and H.A. Makse, Self-similarity of complex networks. *Nature*, **433** (2005) 392-395.
- [2] C.Y. Lee and S. Jung, Statistical self-similar properties of complex networks. *Phys. Rev. E*, **73** (2006) 066102.
- [3] L. Guo and X. Cai, The fractal dimensions of complex networks. *Chinese Phys. Lett.*, **26** (2009) 088901.
- [4] P. Erdos and A. Renyi, On the evolution of random graphs. *Publ. Math. Inst. Hung. Acad. Sci.*, **5** (1960) 17-61.
- [5] S. Milgram, The small-world problem. *Psychol. Today*, **2** (1967) 60-67.

- [6] R. Albert, H. Jeong and A.L. Barabasi, Diameter of the World Wide Web. *Nature*, **401** (1999) 130-131.
- [7] R. Albert and A.L. Barabasi, Statistical mechanics of complex networks. *Rev. Mod. Phys.*, **74** (2002) 47-97.
- [8] M. Faloutsos, P. Faloutsos and C. Faloutsos, On power-law relationships of the internet topology. *Comput. Commun. Rev.*, **29** (1999) 251-262.
- [9] B.B. Mandelbrot, *The fractal Geometry of Nature* (Freeman, New York, 1983).
- [10] J. Feder, *Fractals* (Plenum, New York, 1988).
- [11] K. Falconer, *Techniques in Fractal Geometry* (Wiley, New York, 1997).
- [12] C. Song, L.K. Gallos, S. Havlin and H.A. Makse, How to calculate the fractal dimension of a complex network: the box covering algorithm. *J. Stat. Mech.: Theor. Exper.*, **3** (2007) P03006.
- [13] J.S. Kim, K.I. Goh, G. Salvi, E. Oh, B. Kahng, and D. Kim, Fractality in complex networks: Critical and supercritical skeletons. *Phys. Rev. E*, **75** (2007) 016110.
- [14] W.X. Zhou, Z.Q. Jiang and D. Sornette, Exploring self-similarity of complex cellular networks: The edge-covering method with simulated annealing and log-periodic sampling. *Physica A*, **375** (2007) 741-752.
- [15] L. Gao, Y. Hu and Z. Di, Accuracy of the ball-covering approach for fractal dimensions of complex networks and a rank-driven algorithm. *Phys. Rev. E*, **78** (2008) 046109.
- [16] O. Shanker, Defining dimension of a complex network. *Mod. Phys. Lett.B*, **21** (2007) 321-326.
- [17] P. Grassberger and I. Procaccia, Characterization of strange attractors. *Phys. Rev. Lett.*, **50** (1983) 346-349.
- [18] T.C. Halsey, M.H. Jensen, L.P. Kadanoff, I. Procaccia, and B.I. Shraiman, Fractal measures and their singularities: the characterization of strange sets. *Phys. Rev. A*, **33** (1986) 1141-1151.
- [19] E. Canessa, Multifractality in time series. *J. Phys. A: Math. Gen.* **33** (2000) 3637-3651.
- [20] V.V. Anh, Q.M. Tieng and Y.K. Tse, Cointegration of stochastic multifractals with application to foreign exchange rates. *Int. Trans. Oper. Res.*, **7** (2000) 349-363.

- [21] Z.G. Yu, V. Anh and K.S. Lau, Multifractal characterisation of length sequences of coding and noncoding segments in a complete genome. *Physica A*, **301** (2001) 351-361.
- [22] Z.G. Yu, V. Anh and K.S. Lau, Measure representation and multifractal analysis of complete genome. *Phys. Rev. E*, **64** (2001) 31903.
- [23] Z.G. Yu, V.V. Anh and B. Wang, Correlation property of length sequences based on global structure of complete genome. *Phys. Rev. E*, **63** (2001) 11903.
- [24] V.V. Anh, K.S. Lau and Z.G. Yu, Recognition of an organism from fragments of its complete genome. *Phys. Rev. E*, **66** (2002) 031910.
- [25] Z.G. Yu, V. Anh and K.S. Lau, Multifractal and correlation analysis of protein sequences from complete genome. *Phys. Rev. E*, **68** (2003) 021913.
- [26] Z.G. Yu, V. Anh and K.S. Lau, Chaos game representation of protein sequences based on the detailed HP model and their multifractal and correlation analyses. *J. Theor. Biol.*, **226** (2004) 341-348.
- [27] L.Q. Zhou, Z.G. Yu, J.Q. Deng, V. Anh and S.C. Long, A fractal method to distinguish coding and noncoding sequences in a complete genome based on a number sequence representation. *J. Theor. Biol.*, **232** (2005) 559-567.
- [28] Z.G. Yu, V.V. Anh, K.S. Lau and L.Q. Zhou, Fractal and multifractal analysis of hydrophobic free energies and solvent accessibilities in proteins. *Phys. Rev. E*, **73** (2006) 031920.
- [29] J.W. Kantelhardt, E. Koscielny-Bunde, D. Rybski, P. Braun, A. Bunde and S. Havlin, Long-term persistence and multifractality of precipitation and river runoff records. *J. Geophys. Res.*, **111** (2006) D01106.
- [30] D. Veneziano, A. Langousis and P. Furcolo, Multifractality and rainfall extremes: A review. *Water Resour. Res.*, **42** (2006) W06D15.
- [31] V. Venugopal, S.G. Roux, E. Foufoula-Georgiou and A. Arneodo, Revisiting multifractality of high-resolution temporal rainfall using a wavelet-based formalism. *Water Resour. Res.*, **42** (2006) W06D14.
- [32] Z.G. Yu, V.V. Anh, J.A. Wanliss and S.M. Watson, Chaos game representation of the Dst index and prediction of geomagnetic storm events, *Chaos, Solitons and Fractals*, **31** (2007) 736-746.
- [33] Z.G. Yu, V. Anh and R. Eastes, Multifractal analysis of geomagnetic storm and solar flare indices and their class dependence. *J. Geophys. Res.*, **114** (2009) A05214.

- [34] Z.G. Yu, V. Anh, Y. Wang, D. Mao and J. Wanliss, Modeling and simulation of the horizontal component of the geomagnetic field by fractional stochastic differential equations in conjunction with empirical mode decomposition. *J. Geophys. Res.*, **115** (2010) A10219,
- [35] K. S. Lau and S. M. Ngai, Multifractal measures and a weak separation condition. *Advances in Mathematics*, **141** (1999) 45-96.
- [36] E.W. Dijkstra, A note on two problems in connexion with graphs. *Numerische Mathematik*, **1** (1959) 269-271.
- [37] M.E.J. Newman, The structure and function of complex networks. *SIAM Review*, **45** (2003) 167-256
- [38] A.L. Barabási and R. Albert, Emergence of scaling in random networks. *Science*, **286** (1999) 509-512.
- [39] M.E.J Newman and D.J. Watts, Renormalization group analysis of the small-world network model. *Phys. Lett.*, **263** (1999) 341-346.
- [40] D.J. Watts and S.H. Strogatz, Collective dynamics of 'small-world' networks. *Nature*, **393** (1998) 440-442.
- [41] J.H.H. Opeusden, M.T.A. Bos, and G. van der Kaaden, Anomalous multifractal spectrum of aggregating Lennard-Jones particles with Brownian dynamics. *Physica A*, **227** (1996) 183-196.
- [42] T.G. Smith and G.D. Lange, Biological cellular morphometry-fractal dimensions, lacunarity and multifractals. in *Fractal in Biology and Medicine* (Birkhäuser, Basel, 1998).
- [43] E. Fernández, J.A. Bolea, G. Ortega and E. Louis, Are neurons multifractals? in *Journal of Neuroscience Methods*, **89** (1999) 151-157.
- [44] Cytoscape software: <http://cytoscapeweb.cytoscape.org/>
- [45] BioGRID: <http://thebiogrid.org/download.php>
- [46] DIP: <http://dip.doe-mbi.ucla.edu/dip/Download.cgi>
- [47] E. Lee, H. Jung, P. Radivojac, J.W. Kim and D. Lee, Analysis of AML genes in dysregulated molecular networks. *BMC Bioinformatics*, **10** (Suppl 2) (2009) S2.

Table 1: Comparison of different scale-free networks

Number of nodes	Number of edges	Diameter	γ	Max(Dq)	Lim(Dq)	ΔDq
500	499	13	1.94 ± 0.02	2.67	1.36	1.31
1000	999	16	2.02 ± 0.07	2.93	1.47	1.46
1500	1499	17	2.09 ± 0.04	2.96	1.65	1.30
2000	1999	20	1.99 ± 0.08	3.05	1.76	1.29
3000	2999	20	2.06 ± 0.04	3.26	1.83	1.44
4000	3999	23	2.09 ± 0.03	3.32	1.80	1.52
5000	4999	23	2.08 ± 0.04	3.26	1.75	1.51
6000	5999	22	2.06 ± 0.04	3.39	1.88	1.51
7000	5999	28	2.08 ± 0.04	3.39	2.10	1.29
8000	5999	25	1.91 ± 0.12	3.33	2.11	1.22

Table 2: Comparison of different small-world networks and regular networks with 5000 nodes

Number of nodes	Number of edges	Diameter	p	Max(Dq)	Lim(Dq)	ΔDq
5000	25159	33	0.03	2.31	2.28	0.03
5000	25207	29	0.04	2.43	2.37	0.06
5000	25290	23	0.06	2.56	2.53	0.03
5000	25358	23	0.08	2.66	2.63	0.03
5000	25513	18	0.1	2.81	2.75	0.06
5000	25621	15	0.13	2.89	2.83	0.06
5000	25792	15	0.15	2.99	2.93	0.06
5000	26017	12	0.2	3.08	3.04	0.04
regular network 5000	250000	50	0	1	1	0.00

Table 3: Comparison of different random networks

Number of nodes	Number of edges	Diameter	p	Max(Dq)	Lim(Dq)	ΔDq
449	610	15	0.005	2.42	2.14	0.28
994	2502	8	0.005	3.32	2.87	0.45
1991	5939	9	0.003	3.73	3.41	0.32
2484	6310	11	0.002	3.70	3.33	0.37
2790	4374	18	0.001	3.29	2.95	0.34
3373	5978	15	0.001	3.47	3.15	0.32
3931	8125	13	0.001	3.67	3.35	0.31
4919	10179	13	0.0008	3.78	3.39	0.39
5620	8804	16	0.00058	3.54	3.21	0.33

Table 4: Comparison of different PPI networks

Networks	Number of nodes	Number of edges	Diameter	D_0	Max(Dq)	Lim(Dq)	ΔDq
Human	8934	41341	14	2.34	4.89	2.65	2.24
Drosophila Melanogaster	7476	26534	11	2.34	4.84	2.87	1.97
S. cerevisiae	4976	21875	10	2.36	4.62	2.48	2.14
E.coli	2516	11465	12	2.14	4.15	2.10	2.05
H.pylori	686	1351	9	2.27	3.47	1.91	1.56
C.elegans	3343	6437	13	2.28	4.47	1.49	2.98
Arabidopsis Thaliana	1298	2767	25	1.83	2.51	1.62	0.89

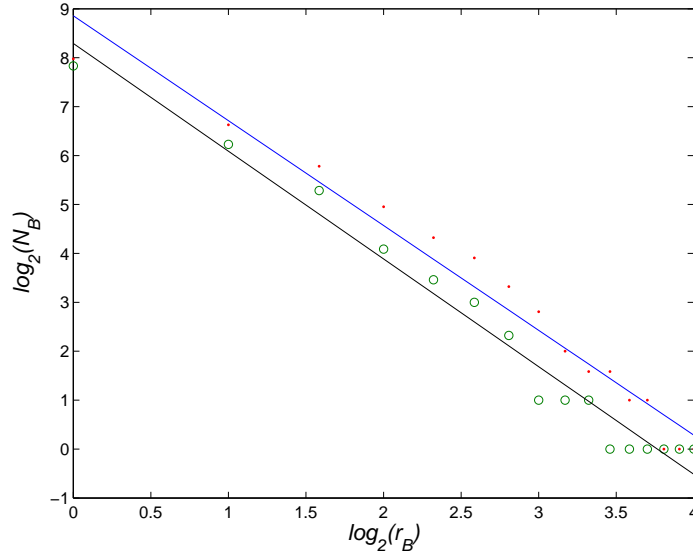


Figure 1: Fractal scaling of the human PPI network (o) and its skeleton (.). The fractal dimension is the absolute value of the slope of each linear fit, which is 2.20 ± 0.09 for the original network and 2.07 ± 0.09 for its skeleton.

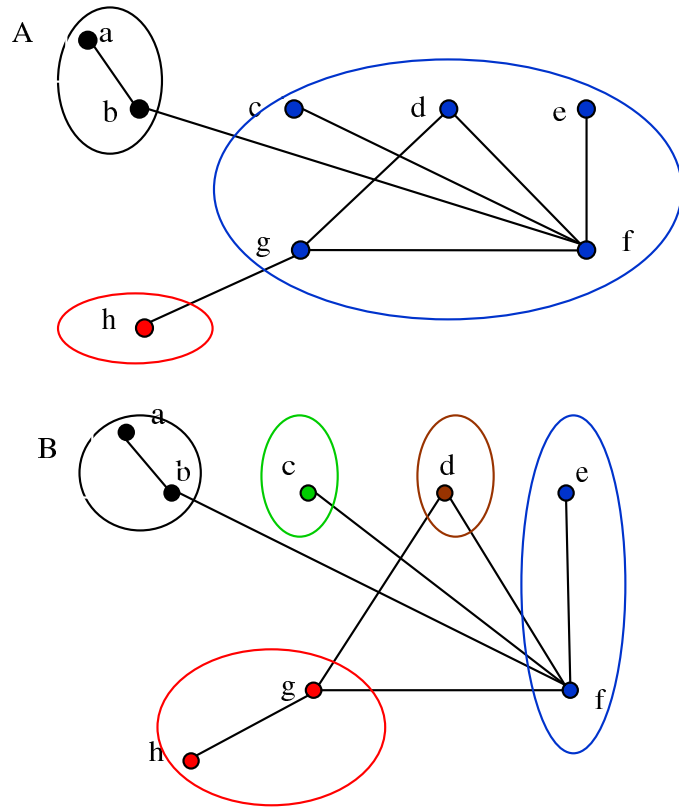


Figure 2: The traditional box-counting algorithm may result in different numbers of boxes needed to cover the entire network.

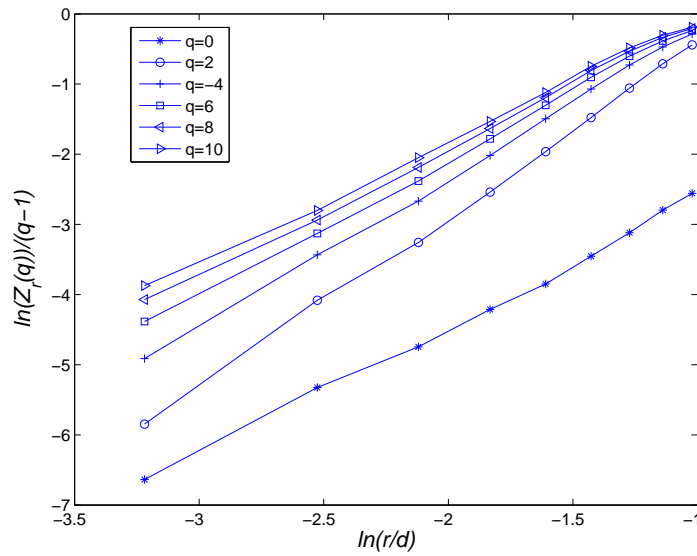


Figure 3: Linear regressions of the Arabidopsis Thaliana PPI network.

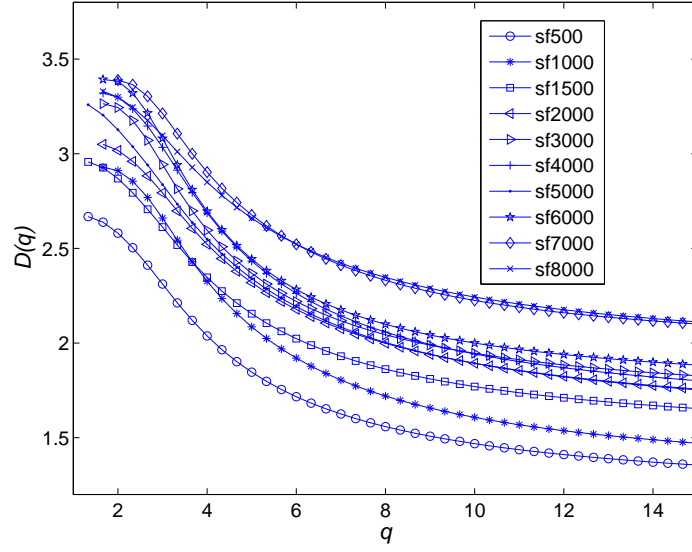


Figure 4: The D_q curves for theoretically generated scale-free networks.

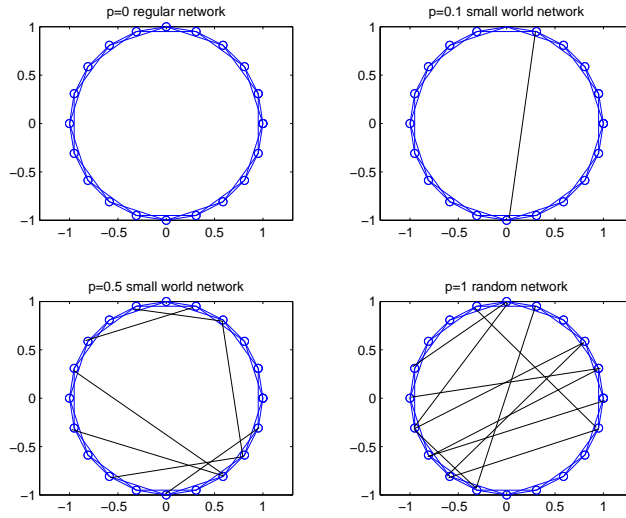


Figure 5: Generation of small-world networks by the NW model.

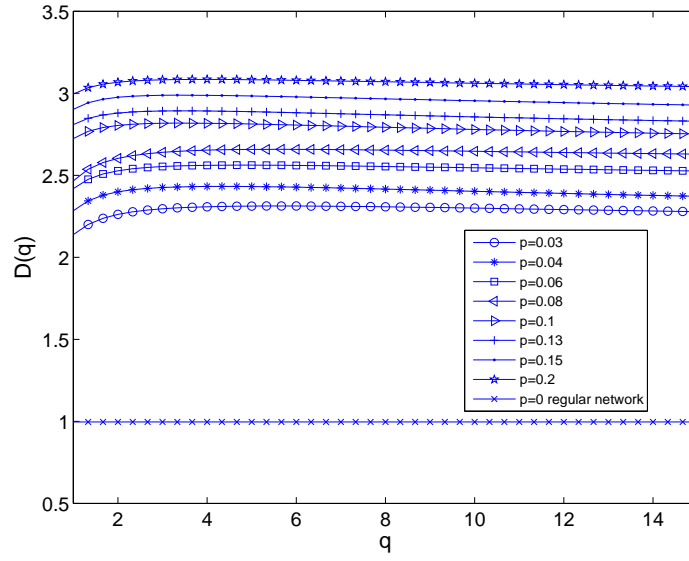


Figure 6: The D_q curves for theoretically generated small-world networks.

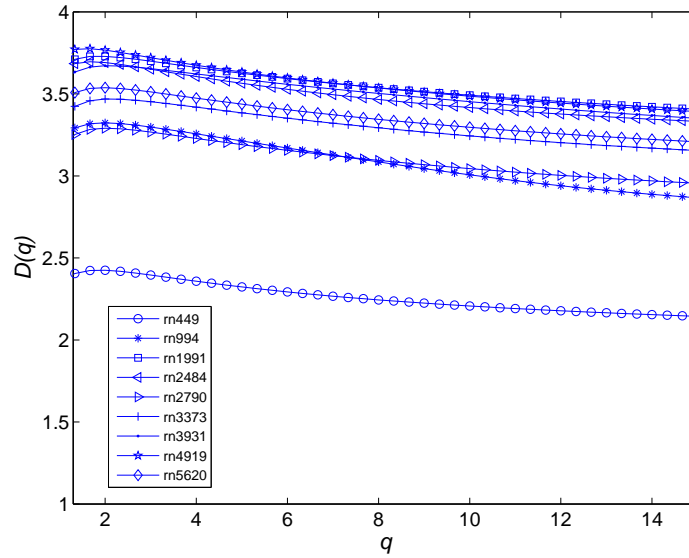


Figure 7: The D_q curves for different random networks.

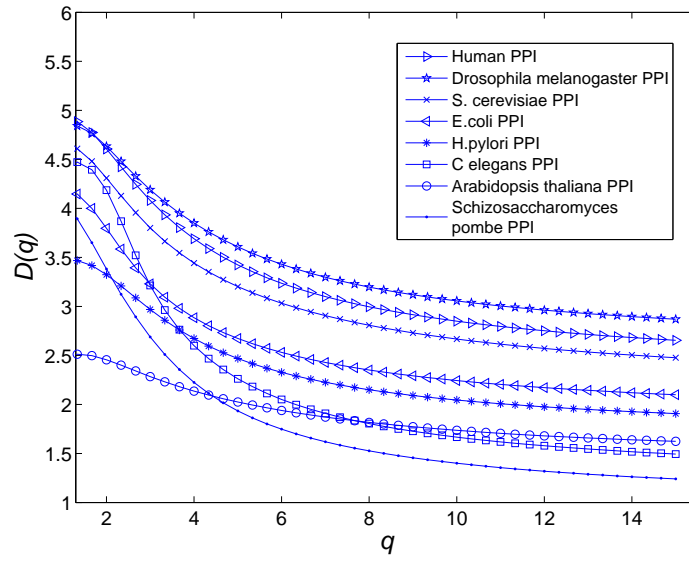


Figure 8: The D_q curves for different PPI networks.